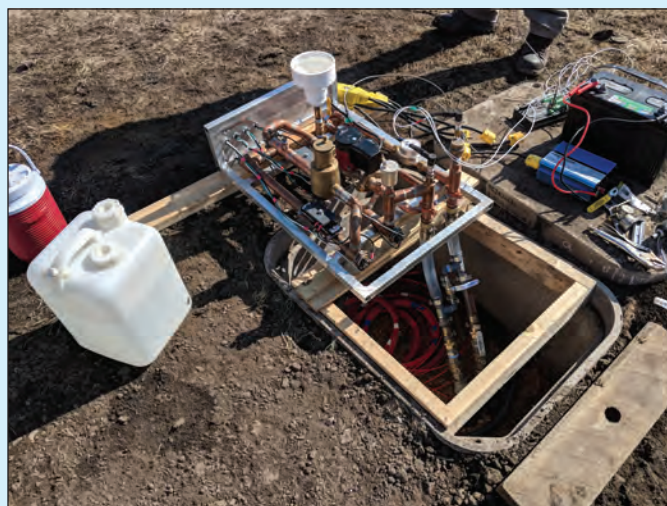
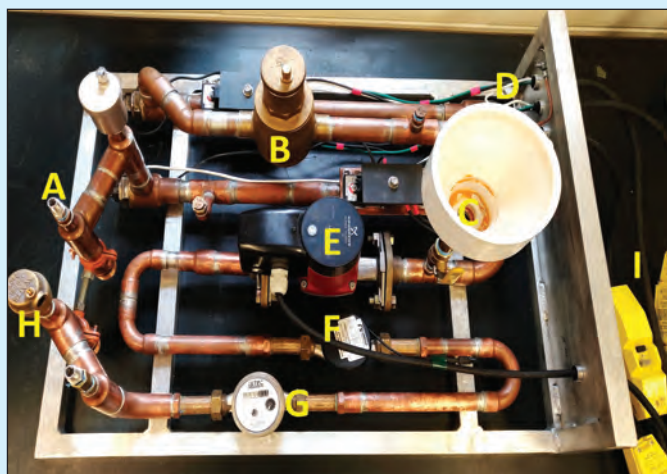


# User's Manual for the Portable Thermal Response Test Device

Yu-Feng F. Lin,<sup>1,2</sup> Chien-Yung Tseng,<sup>1,2</sup> and Steve L. Sargent<sup>1</sup>

<sup>1</sup>Illinois State Geological Survey, Prairie Research Institute, University of Illinois at Urbana-Champaign

<sup>2</sup>Department of Civil and Environmental Engineering, University of Illinois at Urbana-Champaign



Circular 603 2020

ILLINOIS STATE GEOLOGICAL SURVEY  
Prairie Research Institute  
University of Illinois at Urbana-Champaign

**I ILLINOIS**  
Illinois State Geological Survey  
PRAIRIE RESEARCH INSTITUTE

**Front cover:** (Top left) The thermal response test device; (top right) the ISTEK mechanical water flowmeter (left) and the OMEGA digital water flowmeter (right); (bottom left) field operation of the portable thermal response test device; (bottom right) Geothermal Research Station at the University of Illinois Energy Farm.



# User's Manual for the Portable Thermal Response Test Device

Yu-Feng F. Lin,<sup>1,2</sup> Chien-Yung Tseng,<sup>1,2</sup> and Steve L. Sargent<sup>1</sup>

<sup>1</sup>Illinois State Geological Survey, Prairie Research Institute, University of Illinois at Urbana-Champaign

<sup>2</sup>Department of Civil and Environmental Engineering, University of Illinois at Urbana-Champaign

**Circular 603 2020**

**ILLINOIS STATE GEOLOGICAL SURVEY**

Prairie Research Institute  
University of Illinois at Urbana-Champaign  
615 E. Peabody Drive  
Champaign, Illinois 61820-6918  
<http://www.isgs.illinois.edu>



Illinois State Geological Survey  
PRAIRIE RESEARCH INSTITUTE

**Suggested citation:**

Lin, Y.-F., C.-Y. Tseng, and S.L. Sargent, 2020, User's manual for the portable thermal response test device: Illinois State Geological Survey, Circular 603, 11 p.

## Contents

|  |    |
|--|----|
| <b>Abstract</b>  | 1  |
| <b>Introduction</b>  | 1  |
| <b>Model Analysis Theory</b>   | 2  |
| <b>The Improved Portable Thermal Response Test Device</b>  | 3  |
| <b>Operational Procedure</b>   | 4  |
| <b>Test Case Analysis</b>  | 8  |
| <b>Conclusions</b>   | 11 |
| <b>Acknowledgments</b>   | 11 |
| <b>References</b>  | 11 |
| <b>Figures</b>   |    |
| 1 Setup of the borehole heat exchange system for the thermal response test (TRT)   | 1  |
| 2 The thermal response test device   | 3  |
| 3 Magnification of the inlet and outlet regions of the thermal response test device, labeled A and H in Figure 2                       | 3  |
| 4 The PT100 precision temperature sensor shown in Figure 3   | 4  |
| 5 Detail of the air eliminator with the floater inside, labeled B in Figure 2  | 4  |
| 6 The SGSR-1203 AP10874GH3 water heater element, labeled D in Figure 2   | 5  |
| 7 A Southwire Company circuit interrupter with a 120VAC (volts alternating current) voltage rating, labeled I in Figure 2              | 5  |
| 8 The thermal cutoff device used to set up the temperature tolerance for the circulating water, to protect the device from overheating | 6  |
| 9 The Grundfos ALPHA2 multispeed pump used to control the flow rate through the loop, labeled E in Figure 2                            | 6  |
| 10 The ISTECH mechanical water flowmeter (left) and the OMEGA digital water flowmeter (right), labeled G and F in Figure 2             | 7  |
| 11 Workflow for operating the portable thermal response test (TRT) device  | 7  |
| 12 Field operation of the portable thermal response test device  | 9  |
| 13 Geothermal Research Station at the University of Illinois Energy Farm (site coordinates lat 40.066202°N, long 88.207597°W)          | 9  |
| 14 Raw data from the 96-h (4-d) thermal response test (TRT)  | 10 |
| 15 Semi-natural-log plot of the 96-h (4-d) thermal response test (TRT)   | 10 |
| 16 Results of the ordinary least squares linear regression for the 96-h (4-d) thermal response test (TRT)                              | 11 |



## ABSTRACT

The thermal response test (TRT) is widely applied to determine geothermal properties, such as geothermal conductivity ( $k$ ) and geothermal resistance ( $R$ ). The TRT works on the principle that the mean temperature change caused by heated circulating water can be measured through the ground over time. The temperature response is due to heat transfer from the heated inflow to the borehole heat exchanger. This temperature response can provide us with an extrapolated prediction of the geothermal performance. The present report outlines a comprehensive workflow for operating the TRT device based on model analysis theory, and it illustrates a test case of TRT measurement. Our aim is to help future users of the TRT device learn to use the device to conduct a basic analysis of raw data from shallow geothermal heat exchange-related projects and to apply this test in both scientific research and educational programs.

## INTRODUCTION

The thermal response test (TRT) is a technology that has been widely applied to measure the thermal characteristics of an underground heat source, such as geothermal conductivity ( $k$ ) and thermal resistance ( $R$ ; Gehlin 2002; Sanner et al. 2005), which are important parameters for designing ground heat exchangers, such as in a borehole ground source heat pump system (Sanner et al., 2000). Because in situ geothermal properties are difficult to measure directly, the TRT is designed to determine the effective thermal parameters indirectly by measuring the mean temperature change of inlet and outlet flows over time. The concept of the TRT method was first proposed by Mogensen (1983), who devised an experimental method to determine the thermal resistance of an entire borehole system. This method was later introduced in the United States (Austin 1998) and Sweden (Eklöf and Gehlin 1996) in the 1990s and was used to develop a mobile TRT device, which is commonly used today. When using the mobile TRT device, the ground and entire borehole system are treated as homogeneously thermally conductive. This assumes that the heat is transferred as a purely conductive process in the ground, without any disturbance from groundwater flow or buoyancy-driven

advection. Therefore, the device measures characteristic quantities of the entire borehole ground system, which are called “effective” thermal properties, such as effective geothermal conductivity ( $k^*$ ), effective geothermal diffusivity ( $\alpha^*$ ), and effective borehole thermal resistance ( $R_b^*$ ). In the 2000s, this mobile TRT device developed rapidly in North America and Europe. It has since been widely applied to measure borehole heat exchange systems in situ by using various analytical and numerical models to estimate the geothermal properties (Spitler 2005; Esen and Inalli 2009).

The typical setup of a borehole heat exchange system with a TRT device includes three main components, as illustrated in Figure 1: the TRT device, a pipe, and the borehole. Inside the borehole, grout is often used to fill the space around the pipe. The thermal conductivity of the grout material is usually similar to the surrounding soil [typically ranging from 0.54 to 1.62 W/(m·K); Austin 1998], which allows the borehole system to be treated as a whole when estimating the effective thermal properties (e.g.,  $k^*$ ,  $\alpha^*$ , and  $R_b^*$ ). As mentioned, these properties can be used to represent the actual geothermal performance (see details in the Model Analysis Theory section).

In this manual, we (1) present newly developed, comprehensive procedures for operating an improved portable TRT device, (2) introduce the basic analytical theory, and (3) illustrate the operational procedures with a test case. The new portable TRT device is significantly reduced in size and weight, and instead of the need for a trailer and vehicle to transport the mobile device, it can be transported by people. Our aim is to build a fundamental workflow to work with the present TRT technology that can be applied to both scientific research studies and educational programs. The objective of this report is to help future users learn to use the device to conduct a basic analysis from the raw data when applying the procedure in geothermal-related projects. For instance, an advanced TRT method, referred to as distributed thermal response testing, was recently developed by coupling the previous prototype version of this TRT device with a fiber-optic distributed temperature sensing system to characterize the geothermal properties of a heterogeneous lithology (McDaniel et al. 2018). Here we include conceptual knowledge of the TRT technology (Introduction), the model analysis theory (Model Analysis Theory section), a description of the device structure (The Improved Portable Thermal Response

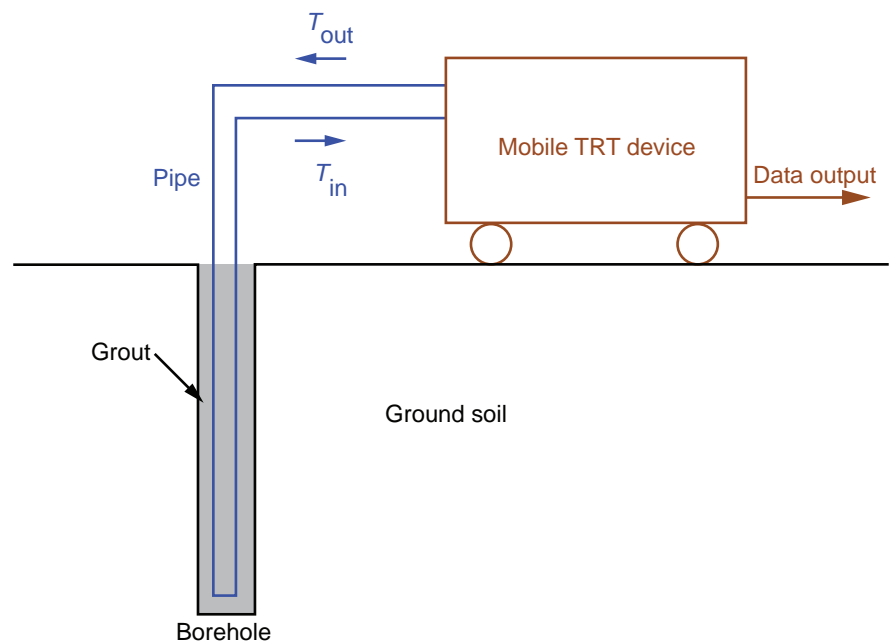


**Figure 1** Setup of the borehole heat exchange system for the thermal response test (TRT).

Test Device section), operational procedures (Operational Procedures section), and an analysis of a test case (Test Case Analysis section).

## MODEL ANALYSIS THEORY

The TRT device works by circulating heated water through the ground. The temperature response is a heating or cooling process that occurs as heat is transferred from the heated inflow to the borehole heat exchanger and then from the outflow back into the TRT device at a different temperature. By measuring the mean temperature change of the inflow and outflow water over time, representing the change in ground temperature, we can obtain information on properties such as the thermal conductivity ( $k$ ) and thermal resistance ( $R$ ) of the borehole heat exchanger. Hence, this temperature response can provide an extrapolated prediction of the borehole performance. Because the TRT technology has developed rapidly over the last two decades, a number of analytical and numerical models have been developed according to the following basic assumptions (Gehlin and Hellstrom 2003; Spitler and Gehlin 2015):

1. Heat transfer underground is purely conductive, uniform, and quasi-steady, and thus can be estimated by the effective geothermal conductivity ( $k^*$ ), the effective geothermal diffusivity ( $\alpha^*$ ), and the effective borehole thermal resistance ( $R_b^*$ ).
2. The geothermal loop connected to the TRT device is radial symmetric to the borehole axis.
3. The heat conducted along the borehole axis is negligible.
4. The mean fluid temperature within the borehole can be treated as a simple average of the inlet and outlet water temperatures.

The simplest model to apply when analyzing the TRT data is the line source model, also known as the Kelvin line source theory. This model assumes that the pipe is as thin as a line (i.e., that the borehole depth is considerably larger than the borehole radius) and perfectly thermally conductive. The theory was first proposed by William Thomson based on the previous theoretical work by Lord Kelvin (Thomson 1884) and was further developed by H.S. Carslaw and

J.C. Jaeger (1959, p. 261–262). When the heating process begins, the heated fluid acts as a constant heat source input into the ground. A fluid heat transfer equation for the temperature field can be used to evaluate the change in the mean temperature difference over time (Equation 1 below), where  $T_{\text{avg}}(t)$  is an average of the inlet and outlet water temperature (K);  $T_i$  is the undisturbed ground temperature (initial fluid temperature, K);  $Q$  is the heat output power (W);  $k^*$  is the effective geothermal conductivity [W/(m·K)];  $H^*$  is the effective borehole depth (m);  $R_b^*$  is the effective borehole thermal resistance [(K·m)/W] between the fluid and the borehole wall; and  $E_1$  is the so-called exponential integral, which is a function of time  $t$  (Equation 2 below), where  $r$  is the radial distance from the line source (borehole center, m) and  $\alpha^*$  is the effective geothermal diffusivity (m/s<sup>2</sup>). The exponential integral  $E_1$  can be written as the approximated expansion (Abramowitz and Stegun 1964; Gehlin and Hellstrom 2003; Equation 3 below), where  $x$  is  $r^2/4\alpha^*t$ ;  $A$  is 0.99999193;  $B$  is 0.24991055;  $D$  is 0.05519968;  $E$  is 0.00976004;  $F$  is 0.00107857; and  $\gamma$  is 0.5772 (Euler's

constant). Carslaw and Jaeger (1959, p. 262) also provided a simplified form of the expansion in Equation 3 (Equation 4 below) when the measurement time  $t$  is long enough ( $t > 5r^2/\alpha^*$ ). This simplified form gives a maximum error of 2.5% when  $t > 20r^2/\alpha^*$  and 10% for  $t > 5r^2/\alpha^*$ . Thus, the fluid heat transfer equation (Equation 1) can be rewritten in a simplified form (Equation 5 below), where  $m$  is the derivative of the mean fluid temperature with respect to  $\ln t$  (Equation 6 below) and  $b$  is the remaining coefficient (Equation 7 below).

The geothermal properties can be estimated according to Equation 5. By analyzing the mean fluid temperature change from the TRT data with respect to time, the slope of the data curve can be used to determine the effective geothermal conductivity (Equation 8 below).

Furthermore, by comparing the difference in temperature with a zero-resistance curve, the effective borehole thermal resistance can be obtained. An example test case data analysis is explained in detail in the Test Case Analysis section.

$$\Delta T(t) = T_{\text{avg}}(t) - T_i = \frac{Q}{4\pi k^* H^*} E_1(t) + \frac{Q}{H^*} R_b^* \quad (1)$$

$$E_1 = \int_1^\infty \frac{e^{-u}}{u} du \quad (2)$$

$$E_1 \approx -\gamma - \ln x + Ax - Bx^2 + Dx^3 - Ex^4 + Fx^5 \quad (3)$$

$$E_1 \approx -\gamma - \ln x = \ln t + \ln \frac{4\alpha^*}{r^2} - 0.5772 \quad (4)$$

$$\Delta T(t) = T_{\text{avg}}(t) - T_i = m(\ln t + b) + \frac{Q}{H^*} R_b^* \quad (5)$$

$$m = \frac{Q}{4\pi k^* H^*} \quad (6)$$

$$b = \ln \frac{4\alpha^*}{r^2} - 0.5772 \quad (7)$$

$$k^* = \frac{Q}{4\pi H^*} \left( \frac{\Delta T}{\ln t} \right)^{-1} \quad (8)$$

## THE IMPROVED PORTABLE THERMAL RESPONSE TEST DEVICE

Improvements to the structure of the TRT device have the objective of reducing the size of the device while maintaining its robustness under field conditions, making it more portable, economical, and effective. The portable TRT device is composed of several parts, as shown in Figure 2.

During circulation, water flows through the borehole pipe and enters the TRT device through the inlet region, labeled A in Figure 2. The inlet and outlet regions are magnified to show detail in Figure 3. Two PT100 precision temperature sensors (Figure 4) are set inside the pipe (Figure 3) to measure the inlet and outlet temperatures. The blue arrows in Figure 3 show the flow directions of inlet and outlet water. Two additional air vents (Figure 3) are designed to release air bubbles, which could affect the test results or cause the device to corrode.

If the air bubbles cannot be fully eliminated through the air vents, then another air eliminator (labeled B in Figure 2) is designed to remove the remaining air generated during water circulation and the temperature change. A cap valve connected to the floater (white plastic disk in Figure 5) will open automatically as the amount of air accumulates, which causes the floater to drop and allows the air to escape from the pipe. As soon as the air has been released from the pipe, the void is replaced with water, which pushes the floater up by buoyancy and closes the valve again.

Water is poured into the pipe through a funnel (labeled C in Figure 2), filling the entire borehole system, including the TRT device. Four water heater elements (Figure 6) are inserted into the tube to heat the circulating water (labeled D in Figure 2).

The heating elements are connected to circuit interrupters (labeled I in Figure 2), which are used for safety to automatically break the circuit when a potentially dangerous wet or overloading environment is detected (Figure 7).

In addition, a thermal cutoff device (Figure 8) is attached directly to the pipe wall to monitor the heat from the heated

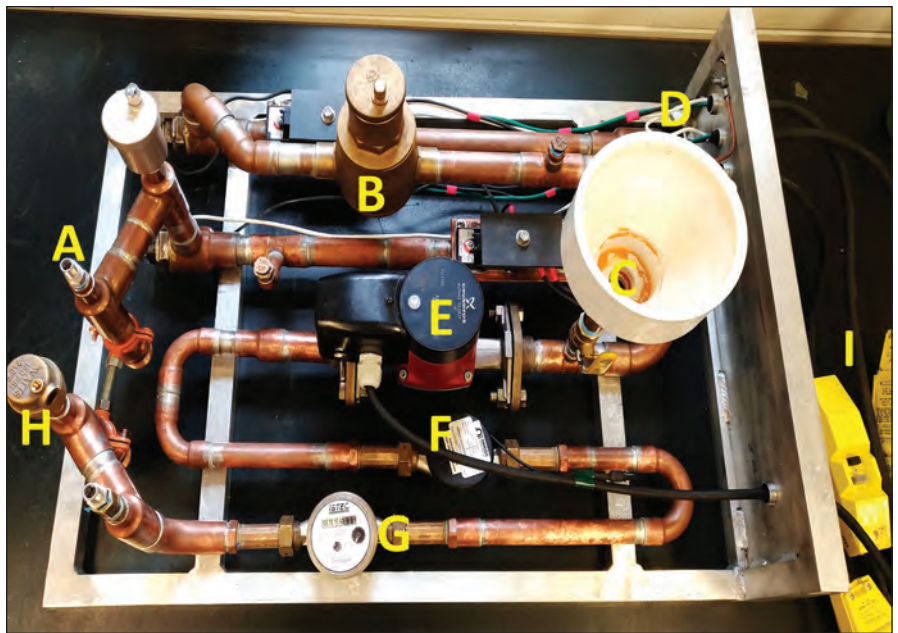


**Figure 2** The thermal response test device. A, inlet region from the borehole pipe; B, air eliminator; C, water input funnel; D, water heater element (the device has four); E, multispeed pump used to drive the circulating water and control the flow rate; F, digital water flowmeter; G, mechanical water flowmeter; H, outlet region to the borehole pipe; I, power strip with circuit interrupter.

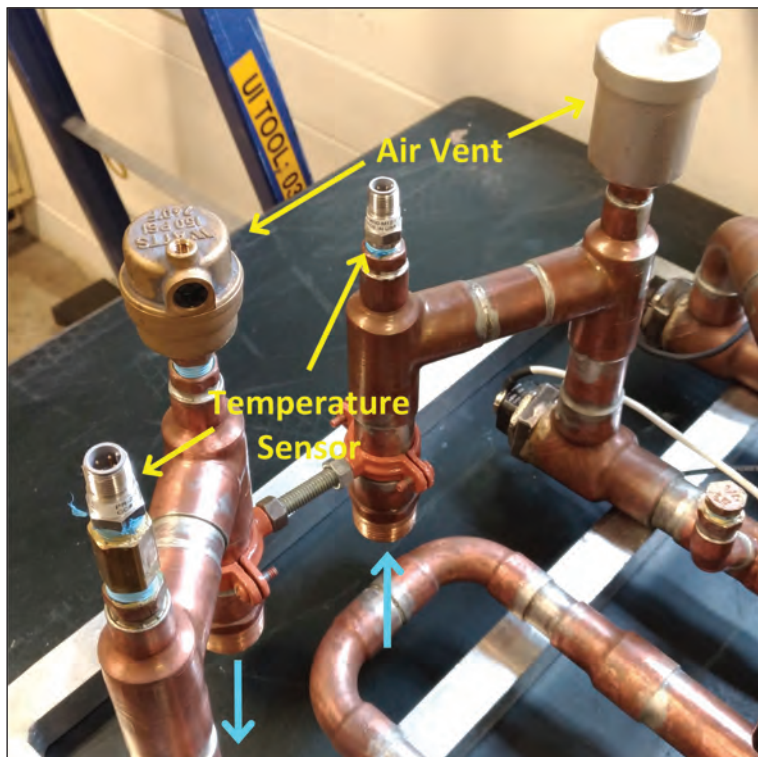


**Figure 3** Magnification of the inlet and outlet regions of the thermal response test device, labeled A and H in Figure 2. The blue arrows show the direction of flow.



**Figure 4** The PT100 precision temperature sensor shown in Figure 3.

water. If the temperature rises over the threshold set by the cutoff device (~45 °C), it will disconnect the heating elements from the electrical power to stop the heating process.

A Grundfos ALPHA2 multispeed pump (Figure 9) is used to control the flow rate through the loop (labeled E in Figure 2).

The circulating water is then pumped into the digital water flowmeter and the mechanical water flowmeter, respectively (labeled F and G in Figure 2; see Figure 10). The digital flowmeter can record the flow rate instantaneously as digital data are transferred to the computer for further analysis, whereas the mechanical flowmeter can display the flow rate instantaneously so that the pump can be adjusted and the circulation flow rate can be controlled.

Finally, the circulating water is pumped back into the borehole pipe through the outlet region (labeled H in Figure 2).

## OPERATIONAL PROCEDURE

In this section, we present a comprehensive list of the steps needed to complete a TRT measurement, along with notes on the process. Figure 11 shows the workflow of the operation.



**Figure 5** Detail of the air eliminator with the floater inside, labeled B in Figure 2.



**Figure 6** The SGSR-1203 AP10874GH3 water heater element, labeled D in Figure 2.



**Figure 7** A Southwire Company circuit interrupter with a 120VAC (volts alternating current) voltage rating, labeled I in Figure 2.

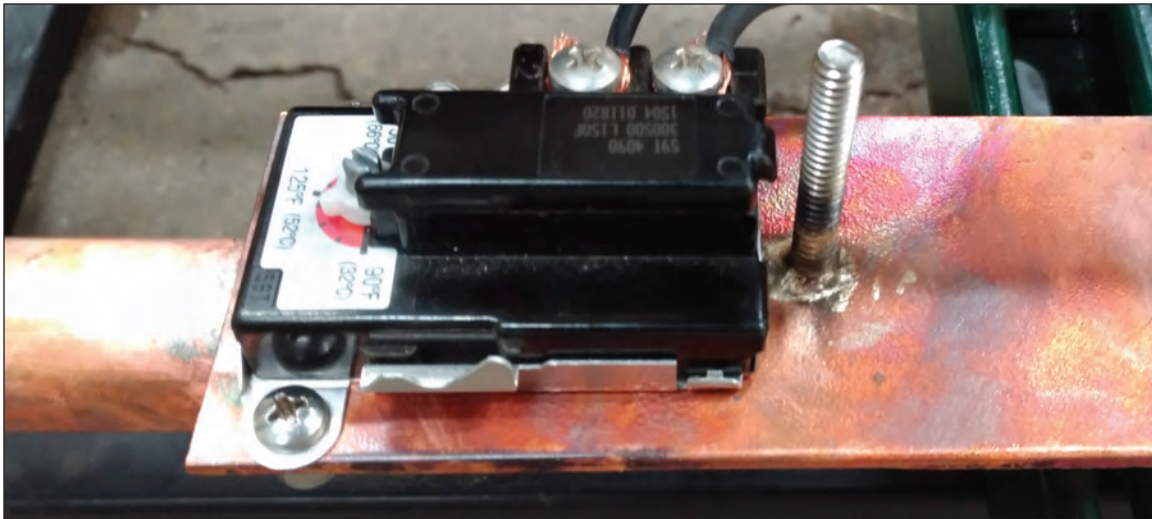


**Figure 8** The thermal cutoff device used to set up the temperature tolerance for the circulating water, to protect the device from overheating.



**Figure 9** The Grundfos ALPHA2 multispeed pump used to control the flow rate through the loop, labeled E in Figure 2. The pump can withstand extreme conditions in the heating system.

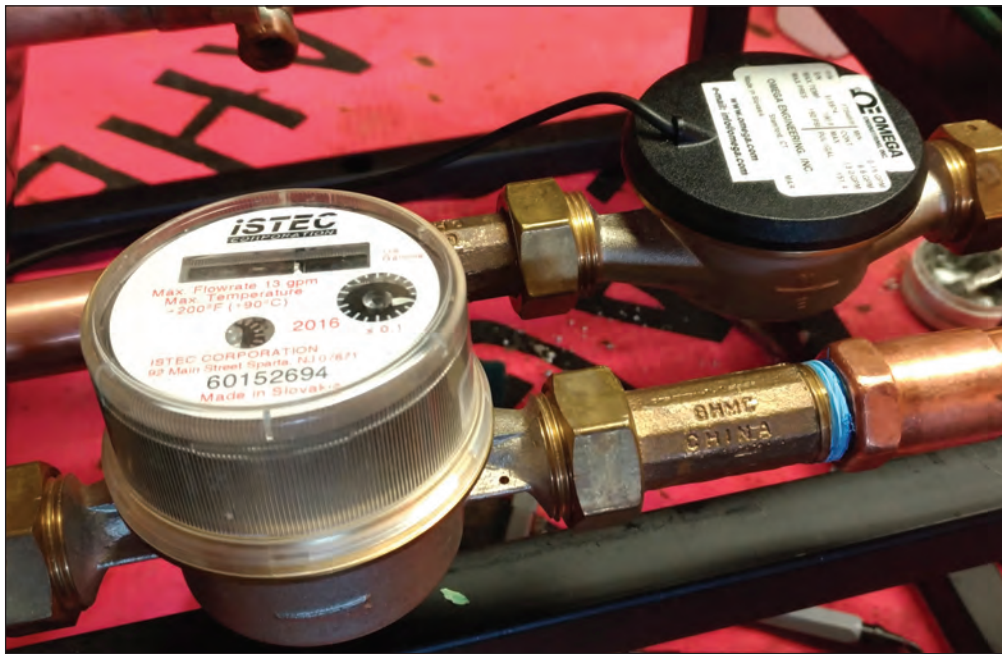


**Figure 10** The ISTECH mechanical water flowmeter (left) and the OMEGA digital water flowmeter (right), labeled G and F in Figure 2.

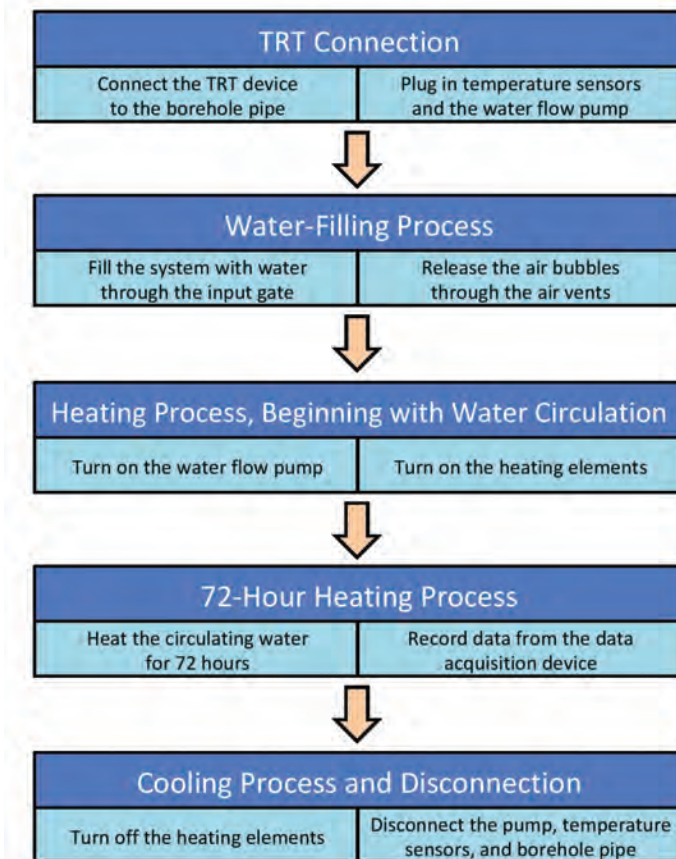


**Figure 11** Workflow for operating the portable thermal response test (TRT) device.

A TRT measurement is conducted according to the following steps:

1. **TRT Connection.** Connect the TRT device to the borehole pipe and plug the temperature sensors and water flow pump into the data acquisition device.
2. **Water-Filling Process.** Fill the portable TRT device and the borehole pipe with water through the water input funnel (labeled C in Figure 2) and release the air bubbles in the pipe through the air vents.
3. **Heating Process, Beginning with Water Circulation.** While the entire borehole system (including the TRT device) is filling with water, turn on the water flow pump to allow the water to circulate for a while (generally 2 to 3 h) so that the water in the TRT device is well mixed with water in the borehole pipe before the heating process begins. Then turn on the heating elements to begin heating the water. Be sure to leave the water-filling funnel open during the heating process to avoid having the heated water expand and overpressure the TRT device. In addition, maintain a constant water flow rate during the entire process.
4. **72-Hour Heating Process.** Wait for at least 72 h until water in the entire borehole system incrementally reaches a stable temperature range (see Model Analysis Theory section). During the heating process, the remaining air bubbles in the device will be released automatically through the air eliminator, and the thermal cutoff device will monitor the temperature of the device. If the circulating water overheats, the thermal cutoff device will disconnect the heating elements from the electrical power to stop the heating process. At the same time, the data acquisition device will be recording the inlet and outlet temperatures via the temperature sensors, and the OMEGA digital water flowmeter will be monitoring the circulating flow rate.
5. **Cooling Process and Disconnection.** After data collection is completed during the heating period, turn off the heating elements and keep the water flow pump running to allow the water to cool. When the water temperature drops below the desired range for the experiment (e.g.,  $<20$  °C), turn

off the water flow pump. Unplug the temperature sensors and the water flow pump from the data acquisition device and disconnect the borehole pipe. Finally, drain the water from the TRT device to finish the entire TRT process.

By following these steps, we were able to obtain a full 72 h of incremental temperature data from the TRT measurement. Figure 12 shows the TRT device operating in the field. In the Test Case Analysis section, we provide an example of test case data to demonstrate how to analyze the raw data and obtain results on the geothermal properties.

## TEST CASE ANALYSIS

A 96-h (4-d) TRT test case measurement was conducted from 2:28 p.m. on June 21, 2018, to 2:30 p.m. on June 25, 2018, at the Geothermal Research Station located at the University of Illinois Energy Farm (site coordinates lat 40.066202°N, long 88.207597°W; Figure 13). The experiment was designed to run longer than 72 h to confirm that the 72-h duration was sufficient. The borehole is 320 ft (~97.5 m) deep and 6.5 in. (~16.5 cm) in diameter. In this section, we describe how to analyze the data measured by the TRT device.

Raw data were obtained with a CR1000 data logger (Campbell Scientific, Logan, Utah), which was used to collect temperature and flow rate measurements from the TRT. The code that drove the data logger was written in Campbell Scientific CRBasic. Figure 14 shows raw data for the temperature change versus time. During the test, the water flow rate was controlled by the water flow pump at 3 gal/min (11.4 L/min), and the total power output of the heating elements was 3,300 W. During the first 2.5 h of the test, the flow pump was active but the water was not heated, which allowed the initial temperature in the system to mix and stabilize. When the heating process began, the rapid increase in outlet temperature caused the average temperature to rise quickly, as shown by the vertical gap in Figure 14. The temperature continued to rise quickly during the first 12 h (before June 22, 2018) and then the rate of increase slowed down (Figure 14). The water temperature finally reached a constant rate of increase after another 12 h (after June 23, 2018; Figure 14).

The time data were replotted on a natural log scale ( $x$ -axis), represented in seconds. The rising water temperature curve in Figure 15 shows an obvious slope change at 24 °C, when time  $t \approx e^{10}$  s (6 h) after the heating process began.

On the basis of the Kelvin line source theory discussed in the Model Analysis Theory section, we extracted the data after time  $t > e^{10}$  s and applied an ordinary least squares linear regression to the data. As shown in Figure 16, the regression result (red dashed line) had an  $R^2$  value of 0.98, the slope of the regression line was 1.46, and the  $y$ -intercept was 9.23.

According to Equation 8 (p. 2) and assuming that the effective depth  $H^*$  is exactly the same as the depth of the borehole pipe (~300 ft [91.5 m]), the estimated effective geothermal conductivity  $k^*$  is approximately 1.97 W/(m·K). This effective geothermal conductivity  $k^*$  value was then added back into Equation 5 (p. 2) and the effective geothermal diffusivity  $\alpha^*$  was set as  $10^{-6}$ , which was within the typical range of the soil geothermal diffusivity (Marquez et al. 2016). By further assuming that the effective radius  $r$  was actually the borehole radius (half the borehole diameter), we could also obtain the estimated effective borehole thermal resistance  $R_b^*$ , which was approximately 0.58 (K·m)/W.

In sum, the raw data obtained from the TRT test case demonstrated the effectiveness of the test in identifying the final slope of the temperature change within 72 h [before  $\ln(s) = 12.46$ ], as shown in Figure 16. Reasonable values were also successfully obtained for the effective geothermal conductivity  $k^*$  and borehole thermal resistance  $R_b^*$  on the basis of the Kelvin line source theory. However, note that certain assumptions and simplifications were made. For instance, we assumed that the heat transfer underground was purely conductive and uniform; thus, we were able to estimate it by using the effective geothermal properties. Yet geology will never be homogeneous or have uniform thermal properties; at times, we may also need to consider the variance in water content and groundwater flow, which may result in a significant difference in the final estimation. Therefore, the results of the parameter estimation from the TRT data may still need correction to move them closer to

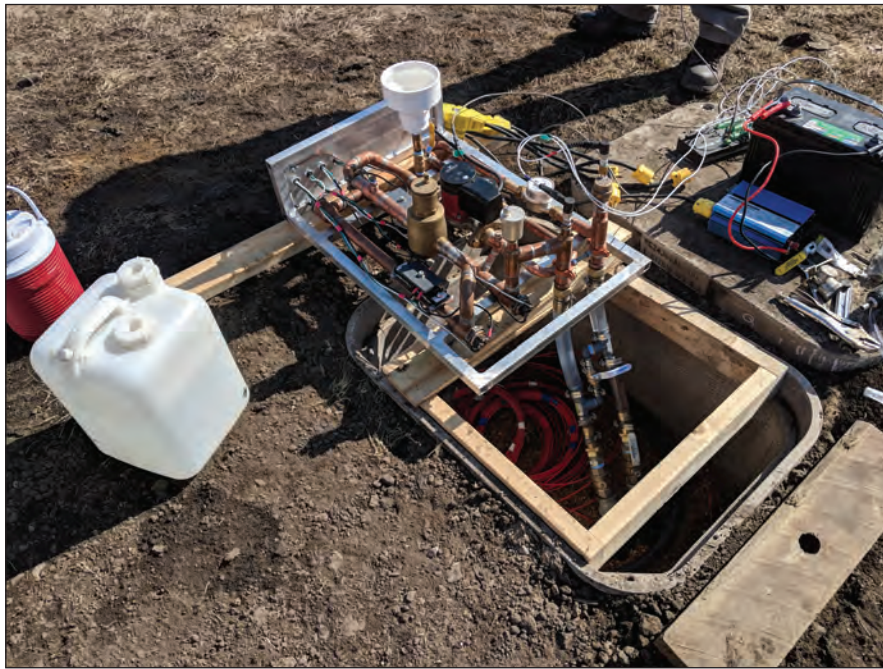


**Figure 12** Field operation of the portable thermal response test device.



**Figure 13** Geothermal Research Station at the University of Illinois Energy Farm (site coordinates lat 40.066202°N, long 88.207597°W). The borehole is 320 ft (~97.5 m) deep and 6.5 in. (~16.5 cm) in diameter.

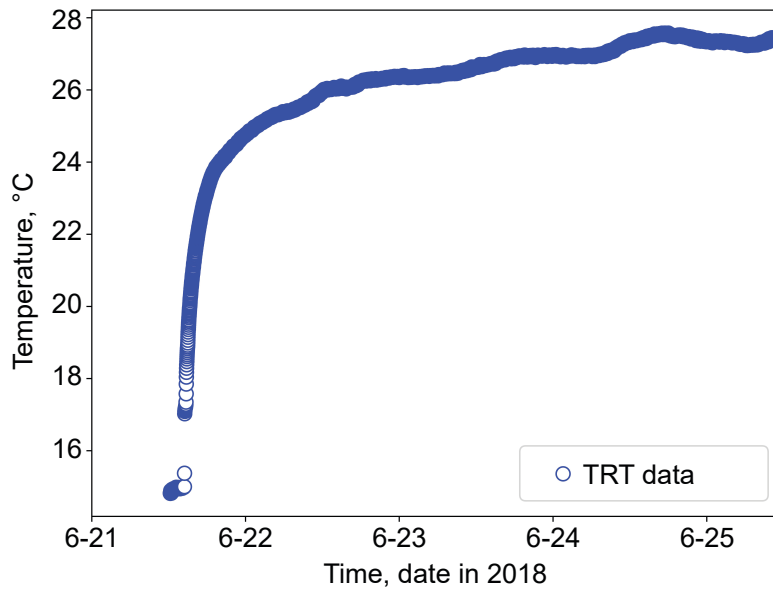


**Figure 14** Raw data from the 96-h (4-d) thermal response test (TRT). The y-axis shows the average of the instantaneously monitored inlet and outlet flow temperatures ( $^{\circ}\text{C}$ ), and the x-axis shows the date (year-month-date).

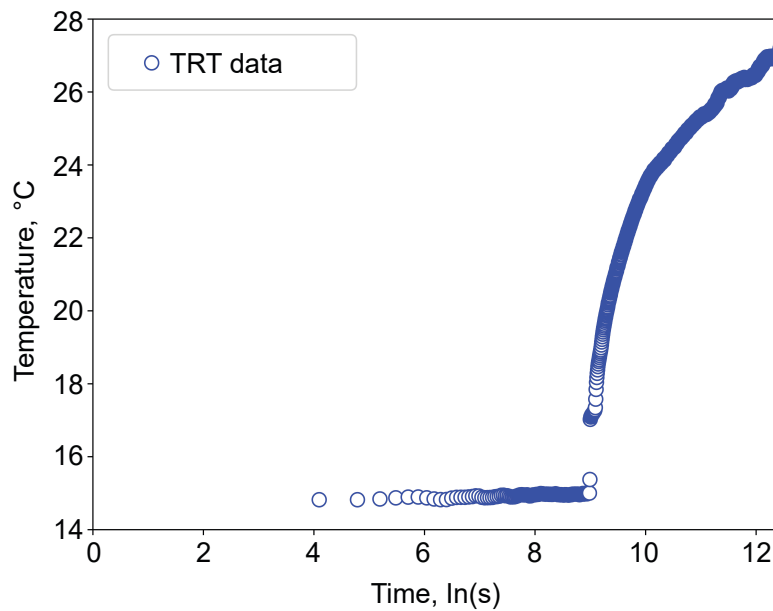


**Figure 15** Semi-natural-log plot of the 96-h (4-d) thermal response test (TRT). The y-axis shows the average of the instantaneously monitored inlet and outlet flow temperatures ( $^{\circ}\text{C}$ ), and the x-axis shows the total testing time (in seconds) at a natural log scale after the heating process began.

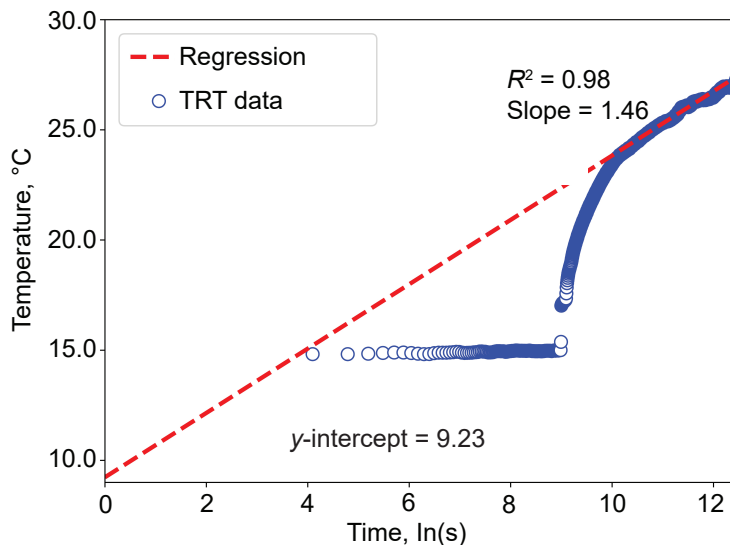


**Figure 16** Results of the ordinary least squares linear regression for the 96-h (4-d) thermal response test (TRT). Raw data are shown by the blue circles, and the regression line is shown by the red dashed line.

real values, which was not within the scope of this report. The distributed thermal response testing mentioned in the Introduction is an example of a more advanced method based on the development of this portable TRT device.

## CONCLUSIONS

This user's manual provides a comprehensive procedure for operating the portable TRT device, along with the related background theories. The example test showed the results from measured data and successfully obtained reasonable values for the effective geothermal conductivity  $k^*$  and effective borehole thermal resistance  $R_b^*$  on the basis of the Kelvin line source theory. In this report, we have outlined a fundamental workflow to help future users learn to use the TRT device and apply it to conduct a basic analysis of raw data from geothermal-related projects in both professional research studies and educational programs.

## ACKNOWLEDGMENTS

The authors acknowledge the generous support of the Student Sustainability Committee and the Energy Farm at the University of Illinois at Urbana-Champaign. We especially thank Adam McDaniel, James Tinjum, and David Hart at the University of Wisconsin for sharing

their experience and providing valuable advice.

## REFERENCES

- Abramowitz, M., and I.A. Stegun, eds., 1964, Handbook of mathematical functions with formulas, graphs, and mathematical tables: Gaithersburg, Maryland, National Bureau of Standards, Applied Mathematics Series 55, 1,046 p.
- Austin, W.A., 1998, Development of an in situ system for measuring ground thermal properties: Stillwater, Oklahoma State University, master's thesis.
- Carlsaw, H.S., and J.C. Jaeger, 1959, Conduction of heat in solids, 2nd ed.: Oxford, UK, Clarendon Press.
- Eklöf, C., and S. Gehlin, 1996, TED—A mobile equipment for thermal response test: Testing and evaluation: Luleå, Sweden, Luleå University of Technology.
- Esen, H., and M. Inalli, 2009, In-situ thermal response test for ground source heat pump system in Elâzığ, Turkey: Energy and Buildings, v. 41, no. 4, p. 395–401.
- Gehlin, S., 2002, Thermal response test: Method development and evaluation: Luleå, Sweden, Luleå University of Technology, PhD dissertation.
- Gehlin, S., and G. Hellstrom, 2003, Comparison of four models for thermal response test evaluation: ASHRAE Transactions, v. 109, p. 131–142.
- Marquez, J.M.A., M.A.M. Bohorquez, and S.G. Melgar, 2016, Ground thermal diffusivity calculation by direct soil temperature measurement: Application to very low enthalpy geothermal energy systems: Sensors (Basel), v. 16, no. 3, p. 306.
- McDaniel, A., J. Tinjum, D.J. Hart, Y.F. Lin, A. Stumpf, and L. Thomas, 2018, Distributed thermal response test to analyze thermal properties in heterogeneous lithology: Geothermics, v. 76, p. 116–124.
- Mogensen, P., 1983, Fluid to duct wall heat transfer in duct system heat storages, in Proceedings of the International Conference on Subsurface Heat Storage in Theory and Practice: Stockholm, Swedish Council for Building Research, p. 652–657.
- Sanner, B., G. Hellstrom, J. Spitler, and S. Gehlin, 2005, Thermal response test—Current status and world-wide application, in Proceedings of the World Geothermal Congress: Bonn, Germany, International Geothermal Association, p. 24–29.
- Sanner, B., M. Reuss, E. Mands, and J. Muller, 2000, Thermal response test—Experiences in Germany, in M. Benner, ed., Proceedings of Terrastock 2000, 8th International Conference on Thermal Energy Storage: Stuttgart, Germany, University of Stuttgart, p. 177–182.
- Spitler, J.D., 2005, Ground-source heat pump system research—Past, present, and future: HVAC&R Research, v. 11, no. 2, p. 165–167.
- Spitler, J.D., and S.E. Gehlin, 2015, Thermal response testing for ground source heat pump systems—An historical review: Renewable and Sustainable Energy Reviews, v. 50, p. 1125–1137.
- Thomson, W., 1884, Compendium of the Fourier mathematics for the conduction of heat in solids, and the mathematically allied physical subjects of diffusion of fluids, and transmission of electric signals through submarine cables: Mathematical and Physical Papers, v. 2, p. 41–60.

